Statistical analysis Data are expressed as mean ± one standard error, unless indicated otherwise. The Statistical Package for the Social Sciences (SPSS; version 11.0; Chicago, IL, USA) was used for the statistical analyses. For univariate comparisons between the patient groups, Student's t test or Mann–Whitney's U test was used, as appropriate, followed by the Bonferroni multiple-comparison test. A value of $p < 0.05$ was considered to indicate statistical significance.

Results

Enrolment and discontinuation The data and safety monitoring board recommended that the study intervention and enrolment be discontinued because of the higher proportion of adverse events (significant elevation in HbA_{1c}) in the ezetimibe group than in the control group. At the time of adverse event analyses, 32 of the targeted 80 patients had been randomly assigned and were included in the safety analyses. In our open-label trial, 32 patients with NAFLD were enrolled. They were randomised to treatment with ezetimibe ($n=17$) or a control ($n=15$) with no significant clinical differences in variables between the groups. Of the 32 randomly assigned patients, 31 had completed the 6 month intervention period; one patient dropped out of the study. One case in the control group withdrew consent after randomisation and before intervention (ESM Fig. 1). The patient who withdrew was excluded from analysis because he did not start his course of treatment. Two analyses were conducted in the remaining patients. In the intention-to-treat analysis (ESM Tables 1 and 2), measures that were missing for participants who discontinued the study were replaced with baseline measures. In the second analysis, the only data included were from participants who completed the study to the end of the 6 month follow-up period. We performed a completed case analysis because there were few dropouts unrelated to baseline values or to their response.

Patient characteristics The 31 study patients (mean age 52.7±2.1 years; mean BMI 29.2±1.0) included 14 randomised to the control group and 17 to the ezetimibe group (ESM Table 3).

At baseline, the characteristics of patients in the ezetimibe and control groups were comparable except for the waist circumference ($p=0.085$) and the Matsuda index ($p=0.060$). The histological features of the liver are summarised in Table 1. At baseline, neither the severity of the individual histological features nor the proportion of patients distributed in the three NAS categories was significantly different between the two groups. All 31 participants agreed to complete the follow-up venous blood samples including OGTT. The ICG15 was conducted in 24 patients (ten control and 14 ezetimibe patients).

Changes in laboratory variables The primary study outcome, serum alanine aminotransferase levels, did not change after ezetimibe treatment (Table 2).

After 6 months of ezetimibe treatment, systolic blood pressure, HbA_{1c}, glycated albumin, and lathosterol were significantly increased, while total cholesterol levels, campesterol, sitosterol and ferritin were significantly decreased. In contrast, body weight, BMI, fasting plasma glucose, plasma γ-glutamyltransferase, triacylglycerols, HDL-cholesterol, small dense LDL (sdLDL), remnant-like particle cholesterol (RLP-C), type IV collagen 7 s levels, NEFA, total bile acid, high-sensitivity C-reactive protein (hsCRP), adiponectin, TNF-α, plasminogen activator inhibitor-1 (PAI-1), 8-isoprostanes and ICG15 did not change after ezetimibe treatment (Table 2). Adipose IR tended to increase in the ezetimibe group (from 88.1±25.5 to 107.5±25.5, $p=0.070$), but not in the control group.

When changes in the groups were compared, the ezetimibe group, but not the control group, had a significant decrease in total cholesterol (ezetimibe, −0.49±0.19 vs control, 0.06±0.14 mmol/l; $p=0.037$), whereas the ezetimibe group, but not control group, showed a significant elevation in HbA_{1c} (ezetimibe, 0.46±0.12% [4.95±1.28 mmol/mol] vs control, 0.08±0.13% [0.78±1.46 mmol/mol]; $p=0.041$). Also, there were significant differences between the groups in cholesterol and HbA_{1c} levels at 6 months. The multiple-comparison

Table 1 Histological characteristics of the livers of patients who completed the study at baseline and 6 months

Variable	Control		p^a	Ezetimibe		p^a	p^b
	Before	After		Before	After		
Steatosis	1.42±0.15	1.17±0.17	0.082	1.56±0.18	1.31±0.15	0.300	0.989
Stage	1.71±0.40	1.71±0.39	1.000	1.75±0.28	1.53±0.26	0.048	0.163
Grade	0.88±0.28	0.79±0.26	0.339	0.84±0.21	0.72±0.15	0.362	0.628
Acinar inflammation	0.88±0.20	0.83±0.20	0.674	1.00±0.13	0.97±0.13	0.751	0.060
Portal inflammation	0.67±0.19	0.71±0.13	0.795	0.44±0.16	0.56±0.16	0.333	0.941
Ballooning	0.58±0.23	0.58±0.23	1.000	0.69±0.20	0.41±0.15	0.045	0.677
NAFLD activity score	3.25±0.53	2.82±0.59	0.139	3.71±0.50	3.06±0.45	0.185	0.705

Data are expressed as the means ± SE

[a] p value for the intergroup comparison (baseline vs 6 month)

[b] p value for the intergroup comparison (changes from baseline between groups)

Table 2 Laboratory values, insulin sensitivity and insulin resistance derived from the euglycaemic insulin clamps and OGTTs of patients who completed the study at baseline and 6 months

Variable	Control			Ezetimibe			
	Before	After	p^a	Before	After	p^a	p^b
Male/female	9/5			11/6			0.232
Age (years)	55.5±3.0			50.4±2.9			
Body weight (kg)	74.4±6.2	73.0±5.6	0.144	81.5±4.6	80.1±4.2	0.367	0.983
BMI (kg/m^2)	27.7±1.7	27.3±1.5	0.172	30.5±1.2	30.0±1.1	0.383	0.999
Waist circumference (cm)	93.1±2.7	92.6±3.4	0.709	99.9±2.5	100.0±2.6	0.956	0.713
Systolic blood pressure (mmHg)	125.2±3.9	126.4±4.9	0.771	124.0±2.4	130.7±2.8	0.048	0.269
Fasting plasma glucose (mmol/l)	7.15±0.63	6.52±0.40	0.240	6.62±0.30	6.87±0.34	0.411	0.131
HbA_{1c} (%)	5.9±0.2	6.0±0.2	0.603	6.1±0.2	6.5±0.2	0.001	0.041
HbA_{1c} (mmol/mol)	40.8±2.2	41.6±2.6	0.603	43.0±2.6	48.0±2.3	0.001	0.041
Hepaplastin test (%)	115.9±5.8	117.1±6.4	0.624	113.7±4.6	111.8±3.7	0.583	0.459
Glycated albumin (%)	15.9±0.8	16.2±1.0	0.397	15.7±0.5	16.8±0.5	0.014	0.196
Serum aspartate aminotransferase (μkat/l)	31.1±4.4	30.3±3.0	0.780	41.8±6.7	33.7±4.1	0.252	0.365
Serum ALT (μkat/l)	37.9±6.8	38.0±4.5	0.978	53.2±8.6	49.3±6.5	0.683	0.723
Plasma γ-glutamyltransferase (μkat/l)	74.9±27.8	65.8±19.5	0.345	71.4±23.4	60.5±16.1	0.220	0.892
Total cholesterol (mmol/l)	5.14±0.21	5.20±0.18	0.672	5.14±0.20	4.65±0.17	0.024	0.037
Triacylglycerols (mmol/l)	1.34±0.12	1.17±0.12	0.105	1.43±0.11	1.46±0.13	0.857	0.303
HDL-C (mmol/l)	1.40±0.08	1.45±0.06	0.914	1.36±0.08	1.36±0.06	0.942	0.903
sdLDL (mmol/l)	0.52±0.07	0.54±0.07	0.782	0.61±0.10	0.50±0.06	0.201	0.251
RLP-C (mmol/l)	0.13±0.01	0.11±0.01	0.163	0.12±0.01	0.11±0.01	0.601	0.365
Lathosterol×10^{-3} (μmol/l)	2.27±0.43	2.85±0.52	0.001	3.52±0.52	5.01±0.67	<0.001	0.018
Campesterol×10^{-3} (μmol/l)	4.32±0.65	6.20±0.68	0.004	3.78±0.42	2.49±0.30	0.007	<0.001
Sitosterol×10^{-3} (μmol/l)	3.04±0.47	3.89±0.39	0.079	2.73±0.28	1.81±0.19	0.004	0.002
Ferritin (pmol/l)	412.1±85.6	235.3±47.0	0.009	395.7±81.3	247.8±56.8	0.005	0.689
Type IV collagen 7 s (μg/l)	4.52±0.48	4.42±0.45	0.622	4.23±0.23	4.33±0.20	0.592	0.465
NEFA (mmol/l)	0.50±0.09	0.63±0.06	0.160	0.51±0.05	0.57±0.03	0.835	0.447
Total bile acid (μmol/l)	12.5±8.0	8.8±5.2	0.214	5.0±0.7	4.8±1.3	0.893	0.267
hsCRP×10^{-3} (μg/ml)	0.12±0.02	0.09±0.02	0.050	0.14±0.04	0.13±0.04	0.886	0.767
Adiponectin (μg/ml)	4.0±0.5	4.6±0.8	0.114	3.0±0.6	3.3±0.6	0.299	0.670
TNF-α ×10^{-5} (pmol/ml)	10.4±2.3	15.6±8.1	0.094	8.1±0.6	30.0±12.7	0.183	0.084
Leptin×10^{-3} (μg/l)	8.1±1.0	9.7±1.3	0.044	10.8±1.4	12.4±1.5	0.085	0.982
PAI-1 (pmol/l)	400.0±44.2	436.5±44.2	0.401	550.0±71.2	488.5±67.3	0.217	0.136
8-Isoprostanes (pmol/mmol creatinine)	76.9±14.3	57.0±8.0	0.147	56.5±6.6	68.0±7.7	0.092	0.031
ICG15 (%)	8.7±2.4	8.5±2.0	0.662	7.7±1.7	7.7±1.5	0.984	0.796
HOMA-IR	10.1±6.5	5.0±2.1	0.471	9.5±2.6	9.3±2.2	0.839	0.479
QUICKI	0.32±0.01	0.33±0.01	0.443	0.30±0.01	0.30±0.01	0.984	0.019
Adipose IR	55.8±15.5	78.8±31.7	0.441	88.1±25.5	107.5±25.5	0.070	0.099
Insulinogenic index	0.43±0.09	0.53±0.11	0.307	0.41±0.08	0.35±0.09	0.501	0.765
H-IR×10^6	1.82±0.46	2.29±0.44	0.568	2.29±0.33	2.66±0.41	0.221	0.796
Matsuda index	3.03±0.45	3.35±0.49	0.368	1.99±0.28	2.01±0.29	0.895	0.013
Muscle insulin sensitivity	0.039±0.006	0.058±0.016	0.210	0.036±0.005	0.034±0.004	0.560	0.067
MCR	4.86±0.50	4.36±0.45	0.174	4.70±0.31	4.80±0.35	0.827	0.352

Data are expressed as means ± SE

[a] p value for the intergroup comparison (baseline vs 6 month)

[b] p value for the intergroup comparison (changes from baseline between groups)

HDL-C, HDL-cholesterol

Table 3 Signalling pathway gene expression changes in the ezetimibe group

Pathway	Gene symbol	Gene name	Affy ID	Up or down	Function
Development_skeletal muscle development	*VEGFA*	Vascular endothelial growth factor A	210512_s_at	Down	Angiogenesis
	ACTA2	Actin, α2, smooth muscle, aorta1	200974_at	Down	Cytoskeleton and cell attachment
	TCF3	Transcription factor 3	209153_s_at	Down	Differentiation
	TTN	Titin	1557994_at	Down	Abundant protein of striated muscle
	TPM2	Tropomyosin 2	204083_s_at	Down	Actin filament binding protein
	MYH11	Myosin, heavy chain 11, smooth muscle	201496_x_at	Down	Smooth muscle myosin
Immune response_phagocytosis	*FYB*	FYN-binding protein	205285_s_at	Up	Platelet activation and IL2 expression
	FCGR3A	Fc fragment of IgG, low affinity IIIA	204006_s_at	Up	ADCC and phagocytosis
	LCP2	Lymphocyte cytosolic protein 2	244251_at	Up	T cell antigen receptor mediated signalling
	CLEC7A	C-type lectin domain family 7, member A	221698_s_at	Up	T cell proliferation
	MSR1	Macrophage scavenger receptor 1	214770_at	Up	Macrophage-associated processes
	FCGR2A	Fc fragment of IgG, low affinity IIA	1565673_at	Up	Promotes phagocytosis
	PRKCB	Protein kinase C, β	209685_s_at	Up	B cell activation, apoptosis induction
	PLCB4	Phospholipase C, β4	240728_at	Up	Inflammation, cell growth, signalling and death
Cell adhesion_integrin priming	*GNA12*	G protein α12	221737_at	Down	Cytoskeletal rearrangement
	ITGB3	Integrin, β3	204628_s_at	Down	Ubiquitously expressed adhesion molecules
	PIK3R2	Phosphoinositide-3-kinase, regulatory subunit 2	229392_s_at	Down	Diverse range of cell functions
Cell adhesion_cadherins	*PTPRF*	Protein tyrosine phosphatase, receptor type, F	200636_s_at	Down	Cell adhesion receptor
	BTRC	β-Transducin repeat containing E3 ubiquitin protein ligase	222374_at	Down	Substrate recognition component of a SCF E3 ubiquitin-protein ligase complex
	CDHR2	Cadherin-related family member 2	220186_s_at	Down	Contact inhibition at the lateral surface of epithelial cells
	SKI	V-ski sarcoma viral oncogene homologue	229265_at	Down	Repressor of TGF-β signalling
	MLLT4	Myeloid/lymphoid or mixed-lineage leukaemia	214939_x_at	Down	Belongs to an adhesion system
	VLDLR	Very low density lipoprotein receptor	209822_s_at	Down	Binds VLDL and transports it into cells by endocytosis
O-Hexadecanoyl-L-carnitine pathway	*TUBB2B*	Tubulin, β 2B class IIB	209372_x_at	Down	Major component of microtubules
	TUBB2A	Tubulin, β2A class IIA	209372_x_at	Down	Major component of microtubules
	PLCE1	Phospholipase C, epsilon 1	205112_at	Down	Hydrolyses phospholipids into fatty acids and other lipophilic molecules
	CPT1B	Carnitine palmitoyltransferase 1B (muscle)	210070_s_at	Down	Rate-controlling enzyme of the long-chain fatty acid β-oxidation pathway
	CPT1A	Carnitine palmitoyltransferase 1A (liver)	203634_s_at	Down	Carnitine-dependent transport across the mitochondrial inner membrane
	NR1H4	Nuclear receptor subfamily 1, group H, member 4	243800_at	Down	Involved in bile acid synthesis and transport.
GalNAcbeta1-3Gal pathway	*PLCB4*	Phospholipase C, β4	240728_at	Up	Formation of inositol 1,4,5-trisphosphate and diacylglycerol
Steroid metabolism_cholesterol biosynthesis	*CYP51A1*	Cytochrome P450, family 51, subfamily A, polypeptide 1	216607_s_at	Up	Transforms lanosterol
	SREBF2	Sterol regulatory element binding transcription factor 2	242748_at	Up	Transcriptional activator required for lipid homeostasis
	SQLE	Squalene epoxidase	209218_at	Up	Catalyses the first oxygenation step in sterol biosynthesis

Table 3 (continued)

Pathway	Gene symbol	Gene name	Affy ID	Up or down	Function
	SC5DL	Sterol-C5-desaturase-like	215064_at	Up	Catalyses the conversion of lathosterol into 7-dehydrocholesterol
	HMGCS1	3-Hydroxy-3-methylglutaryl-CoA synthase 1	205822_s_at	Up	Condenses acetyl-CoA with acetoacetyl-CoA to form HMG-CoA

Bonferroni test revealed highly significant differences in the changes in total cholesterol ($p = 0.037$) and HbA_{1c} ($p = 0.040$) between the ezetimibe and control groups.

Increased concentrations of the cholesterol synthesis markers lathosterol (ezetimibe, 1.49±0.32 nmol/l vs control, 0.58±0.14 nmol/l; $p = 0.018$) and decreased concentrations of the cholesterol absorption markers campesterol (ezetimibe, −1.28±0.41 nmol/l vs control, 1.88±0.54 nmol/l, $p = 0.000$) and sitosterol (ezetimibe, −0.91±0.27 nmol/l vs control, 0.85± 0.45 nmol/l; $p = 0.002$) were observed on treatment. The ezetimibe group had an increase, whereas the control group had a decrease, in the level of 8-isoprostanes (ezetimibe, 11.6± 6.4 pmol/mmol creatinine vs control, −19.9±12.9 pmol/mmol creatinine; $p = 0.031$).

When changes between groups were compared, the ezetimibe group had a greater decrease in the Matsuda index (ezetimibe=−0.78±0.57 vs control=−1.35±0.55, $p = 0.013$), QUICKI (ezetimibe= −0.02±0.01 vs control=0.03±0.0, $p = 0.019$), and muscle insulin sensitivity (ezetimibe= −0.002±0.004 vs control=0.019±0.014, $p = 0.067$) than the control group.

Changes in liver histology Twenty-eight of 31 participants, 16 in the ezetimibe group and 12 in the control group, agreed to complete the follow-up and undergo a liver biopsy at 6 months, allowing for complete case analysis of the data (Table 1). After 6 months, the changes in staging score (from 1.75±0.28 to 1.53±0.26) and ballooning score (from 0.69± 0.20 to 0.41±0.15) were significantly improved in the ezetimibe group compared with the control group, whereas the scores of steatosis, lobular inflammation and NAS were not significantly changed in either group. The degree of all of these histological features was not significantly different between the two groups (Table 1).

Serial changes in liver gene with ezetimibe treatment Gene expression profiling was conducted in samples from nine patients in the ezetimibe group and six in the control group (ESM Table 4). In the ezetimibe group, 434 genes were upregulated and 410 genes downregulated, while in the control group, 643 genes were upregulated and 367 genes downregulated. Pathway analysis of the process network of differentially expressed genes showed coordinate downregulation of genes involved in skeletal muscle development and cell adhesion molecules in the ezetimibe group, suggesting a suppression of stellate cell development into myofibroblasts (Table 3). In addition, ezetimibe activated the immune response pathway. In contrast, genes involved in skeletal muscle development were upregulated and those in the immune response downregulated in the control group (Table 4). Pathway analysis of the metabolic network also revealed decreased L-carnitine pathway and increased steroid metabolism with ezetimibe treatment, but decreased CoA biosynthesis and increased glycerol 3-phosphate pathway in the control group (ESM Fig. 2).

Changes in plasma fatty acid composition and fatty acid composition extracted from liver tissue The changes in plasma fatty acid composition are shown in Table 5. Compared with baseline levels, only eicosatrienoic acid was significantly increased in the ezetimibe group.

Fatty acid composition in extracted liver tissue was available for 16 NAFLD patients treated with ezetimibe and 12 controls (Table 6). Ezetimibe treatment for 6 months significantly and markedly increased hepatic lauric, myristic, palmitic, palmitoleic, margaric and stearic acids compared with the control group. The changes in hepatic fatty acid composition did not correlate with the changes in serum fatty acid composition before and after ezetimibe treatment (ESM Table 5).

Discussion

This is the first report of the efficacy of ezetimibe treatment on liver pathology in patients with NAFLD in an open-label randomised controlled trial. Treatment with 10 mg/day ezetimibe for 6 months did not alter the primary study outcome, serum aminotransferase levels. Ezetimibe significantly decreased serum cholesterol levels and cholesterol absorption markers as expected, whereas, in contrast to previous reports, ezetimibe treatment did not decrease serum levels of triacylglycerol. Our initial hypothesis was that ezetimibe treatment ameliorates liver pathology by inhibiting the absorption of toxic lipids such as oxidised cholesterol and palmitate. In our animal model, cholesterol feeding to mice increased not

Table 4 Signalling pathway gene expression changes in the control group

Pathway	Gene symbol	Gene name	Affy ID	Up or down	Function
Muscle contraction	*MYH11*	Myosin, heavy chain 11, smooth muscle	201497_x_at	Up	Smooth muscle myosin
	CALM1	Calmodulin 1	241619_at	Up	Ion channels and other proteins by Ca^{2+}
	KCNJ15	Potassium inwardly-rectifying channel, subfamily J, member 15	211806_s_at	Up	Integral membrane protein, inward-rectifier type potassium channel
	SRI	Sorcin	208920_at	Up	Modulates excitation–contraction coupling in the heart
	ACTA2	Actin, α2, smooth muscle, aorta	215787_at	Up	Cell motility, structure and integrity
	TTN	Titin	1557994_at	Up	Abundant protein of striated muscle
	EDNRA	Endothelin receptor type A	204463_s_at	Up	Receptor for endothelin-1
	TPM2	Tropomyosin 2	204083_s_at	Up	Actin filament binding protein
	CRYAB	Crystallin, αB	209283_at	Up	Transparency and refractive index of the lens
Development_skeletal muscle development	*GTF2IRD1*	GTF2I repeat domain containing 1	218412_s_at	Up	Transcription regulator involved in cell-cycle progression, skeletal muscle differentiation
	ADAM12	ADAM metallopeptidase domain 12	213790_at	Up	Skeletal muscle regeneration
	MAP1B	Microtubule-associated protein 1B	226084_at	Up	Facilitates tyrosination of α-tubulin in neuronal microtubules
	MYOM1	Myomesin 1	205610_at	Up	Major component of the vertebrate myofibrillar M band
Cell cycle_G1-S growth factor regulation	*DACH1*	Dachshund homologue 1	205472_s_at	Up	Transcription factor that is involved in regulation of organogenesis
	FOXN3	Forkhead box N3	229652_s_at	Up	Transcriptional repressor, DNA damage-inducible cell cycle arrests
	TGFB2	Transforming growth factor, β2	228121_at	Up	Suppressive effects on interleukin-2 dependent T cell growth
	PIK3CD	Phosphatidylinositol-4,5-bisphosphate 3-kinase, catalytic subunit delta	203879_at	Up	Generate PIP3, recruiting PH domain-containing proteins to the membrane
	EGFR	Epidermal growth factor receptor	1565484_x_at	Up	Antagonist of EGF action
	CCNA2	Cyclin A2	203418_at	Up	Control of the cell cycle at the G1/S and the G2/M transitions
	AKT3	v-Akt murine thymoma viral oncogene homologue 3	219393_s_at	Up	Metabolism, proliferation, cell survival, growth and angiogenesis
	PRKD1	Protein kinase D1	205880_at	Up	Converts transient DAG signals into prolonged physiological effects
Regulation of metabolism_	*INSR*	Insulin receptor	226450_at	Down	Pleiotropic actions of insulin
Bile acid regulation of lipid metabolism and	*SLC27A5*	Solute carrier family 27, member 5	219733_s_at	Down	Bile acid metabolism
Negative FXR-dependent regulation of bile acids concentration	*MBTPS2*	Membrane-bound transcription factor peptidase	1554604_at	Down	Intramembrane proteolysis of SREBPs
	PIK3R3	Phosphoinositide-3-kinase, regulatory subunit 3	202743_at	Down	During insulin stimulation, it also binds to IRS-1
	MTTP	Microsomal triacylglycerol transfer protein	205675_at	Down	Catalyses the transport of triglyceride, cholesteryl ester, and phospholipid
	PPARA	Peroxisome proliferator-activated receptor α	226978_at	Down	Ligand-activated transcription factor
	CYP7A1	Cytochrome P450, family 7, subfamily A	207406_at	Down	Catalyses cholesterol catabolism and bile acid biosynthesis
	FOXA3	Forkhead box A3	228463_at	Down	Transcription factor

Table 4 (continued)

Pathway	Gene symbol	Gene name	Affy ID	Up or down	Function
Immune response_phagosome in antigen presentation	*HLA-B*	Major histocompatibility complex, class I, B	211911_x_at	Down	Foreign antigens to the immune system
	CD14	CD14 molecule	201743_at	Down	Mediates the innate immune response to bacterial lipopolysaccharide
	LBP	Lipopolysaccharide binding protein	211652_s_at	Down	Binds to the lipid A moiety of bacterial lipopolysaccharides
	CTSS	Cathepsin S	202901_x_at	Down	Thiol protease
	DERL1	Derlin 1	222543_at	Down	Functional component of endoplasmic reticulum-associated degradation
	CFL2	Cofilin 2	224352_s_at	Down	Reversibly controls actin polymerisation and depolymerisation
	PAK1	p21 protein (Cdc42/Rac)-activated kinase 1	230100_x_at	Down	Activated kinase acts on a variety of targets
Vitamin, mediator and cofactor	*SLC1A2*	Solute carrier family 1, member 2	1558009_at	Down	Transports L-glutamate and also L- and D-aspartate
Metabolism_CoA biosynthesis and transport	*PANK3*	Pantothenate kinase 3	218433_at	Down	Physiological regulation of the intracellular CoA concentration
	PANK1	Pantothenate kinase 1	226649_at	Down	Physiological regulation of the intracellular CoA concentration
	VNN1	Vanin 1	205844_at	Down	Membrane-associated proteins
	ACSL5	Acyl-CoA synthetase long-chain family member 5	222592_s_at	Down	Synthesis of cellular lipids and degradation via β-oxidation
	ACOT1	Acyl-CoA thioesterase 1	202982_s_at	Down	Catalyses the hydrolysis of acyl-CoAs to the NEFA and coenzyme A
	ACOT2	Acyl-CoA thioesterase 2	202982_s_at	Down	Catalyses the hydrolysis of acyl-CoAs to the NEFA and coenzyme A
	ENPP1	Ectonucleotide pyrophosphatase/ phosphodiesterase 1	229088_at	Down	Involved primarily in ATP hydrolysis at the plasma membrane
Phatidic acid pathway	*GPR63*	G protein-coupled receptor 63	220993_s_at	Up	Orphan receptor. May play a role in brain function
2-Oleoyl-glycerol_3-phosphate pathway	*LPAR1*	Lysophosphatidic acid receptor 1	204037_at	Up	Receptor for LPA, a mediator of diverse cellular activities

only cholesterol but also triacylglycerols in the liver, and upregulated the gene for sterol regulatory element binding protein (SREBP)-1c that governs fatty acid synthesis [3], probably via activation of liver-X-receptor (LXR) in the liver [25]. Therefore, in experimental models of high-cholesterol-diet-induced steatohepatitis, ezetimibe ameliorated liver steatosis by reducing cholesterol-induced activation of LXR and SREBP-1c [26, 27]. In the present study, however, treatment with ezetimibe unexpectedly ameliorated liver fibrosis staging and ballooning scores without significantly changing hepatic steatosis and insulin resistance.

One possible explanation for the improvement of hepatic fibrosis by ezetimibe treatment may be related to the direct effect of cholesterol on hepatic fibrogenesis. The cholesterol molecule affects membrane organisation and structure, which are critical determinants of membrane bilayer permeability and fluidity [28]. Altered cholesterol metabolism has several toxic effects on hepatocytes, resident macrophages, Kupffer cells and hepatic stellate cells, which promote NASH through diverse mechanisms. Hepatic stellate cells, in particular, are responsible for liver fibrosis in NASH. It has recently been reported that intracellular cholesterol accumulation directly activates hepatic stellated cells through a toll-like receptor-4-dependent pathway and triggers hepatic fibrosis [29]. These effects might be more evident in humans because, unlike rodents, where NPC1L1 is primarily expressed in the intestine, in humans *NPC1L1* mRNA is highly expressed both in the small intestine and liver. Therefore, ezetimibe is estimated to inhibit not only dietary and biliary cholesterol absorption through the small intestine, but also reabsorption of biliary cholesterol in the liver [30, 31]. Thus, ezetimibe may inhibit liver fibrosis by ameliorating

Table 5 Changes in plasma fatty acid composition

Fatty acid	Control		p^a	Ezetimibe		p^a	p^b
	Before	After		Before	After		
C12:0 (lauric acid)	1.9±0.5	1.2±0.2	0.177	2.3±0.6	2.1±0.5	0.753	0.301
C14:0 (myristic acid)	24.9±2.5	23.6±2.9	0.575	27.1±2.8	29.5±3.7	0.441	0.352
C16:0 (palmitic acid)	698.0±24.7	690.0±38.2	0.827	714.3±32.5	717.0±36.2	0.991	0.893
C16:1n-7 (palmitoleic acid)	68.6±6.5	72.5±9.6	0.643	62.4±5.0	69.9±6.2	0.219	0.721
C17:0 (margaric acid)	NE	NE		NE	NE		
C18:0 (stearic acid)	203.3±9.4	196.7±6.9	0.488	207.2±7.7	211.0±9.9	0.854	0.571
C18:1n-9 (oleic acid)	560.2±31.3	556.4±30.3	0.914	547.3±23.9	578.8±32.1	0.475	0.550
C18:2n-6 (linoleic acid)	745.8±26.3	750.6±34.4	0.910	735.8±34.2	713.5±31.4	0.558	0.629
C18:3n-6 (γ-linolenic acid)	9.8±1.3	9.2±1.0	0.506	9.8±0.9	11.1±1.5	0.402	0.300
C18:3n-3 (α-linolenic acid)	21.7±1.6	20.1±1.4	0.285	23.0±2.2	21.6±1.5	0.507	0.924
C20:0n-6 (arachidic acid)	7.0±0.4	6.9±0.3	0.671	7.2±0.2	7.0±0.3	0.410	0.642
C20:1n-9 (eicosenoic acid)	4.8±0.3	4.8±0.4	0.323	4.3±0.2	4.2±0.3	0.831	0.343
C20:2n-6 (eicosadienoic acid)	6.1±0.4	6.1±0.3	0.899	5.6±0.2	5.7±0.3	0.774	0.770
C20:3n-6 (dihomo-γ-linolenic acid)	36.6±3.0	37.3±2.8	0.784	36.5±2.4	40.6±3.7	0.247	0.438
C20:3n-9 (eicosatrienoic acid)	2.5±0.4	2.4±0.4	0.941	1.9±0.2	2.7±0.5	0.034	0.079
C20:4n-6 (arachidonic acid)	135.7±8.4	138.8±6.0	0.689	143.8±11.1	151.1±11.0	0.538	0.787
C20:5n-3 (eicosapentaenoic acid)	67.0±9.0	71.3±9.3	0.640	64.4±7.2	59.1±5.7	0.385	0.369
C22:0 (behenic acid)	16.6±0.8	18.3±1.0	0.035	17.1±0.8	17.9±1.3	0.623	0.468
C22:1n-9 (erucic acid)	1.6±0.1	1.3±0.1	0.066	1.3±0.1	1.3±0.1	0.914	0.170
C22:2n-6 (docosadienoic acid)	NE	NE		NE	NE		
C22:4n-6 (docosatetraenoic acid)	3.9±0.2	4.2±0.2	0.252	4.4±0.3	4.9±0.6	0.262	0.689
C22:5n-3 (docosapentaenoic acid)	20.0±1.4	20.7±1.7	0.657	20.7±1.7	21.5±1.7	0.839	0.887
C22:6n-3 (docosahexaenoic acid)	128.7±9.8	138.6±9.3	0.231	126.5±10.0	128.3±10.8	0.936	0.456
C24:1 (nervonic acid)	35.4±2.2	36.1±2.1	0.656	31.6±1.8	30.3±1.9	0.275	0.263

Data are expressed as means ± SE

[a] p value for the intergroup comparison (baseline vs 6 month)

[b] p value for the intergroup comparison (changes from baseline between groups)

NE, not estimated

cholesterol-induced activation of hepatic stellate cells in patients with NAFLD. This hypothesis was well supported by the hepatic gene expression profile induced by ezetimibe administration. Ezetimibe treatment coordinately downregulated genes involved in skeletal muscle development and cell adhesion molecules, suggesting that ezetimibe suppressed stellate cell development into myofibroblasts and thereby inhibited fibrogenesis.

Another important finding of the present study was that treatment with ezetimibe significantly deteriorated glycaemic control. Ezetimibe therapy also altered the hepatic profile of fatty acid components by significantly increasing hepatic levels of lauric, myristic, palmitic, palmitoleic, margaric, stearic, oleic and linoleic acids. Experimentally, palmitate induces interleukin-8 [32], endoplasmic reticulum stress, and c-Jun amino-terminal kinase activation and promotes apoptosis in the liver [5, 33, 34]. Lipid-induced oxidative stress and inflammation are closely related to insulin resistance [3, 5], which could be relevant to the ezetimibe-induced deterioration of glucose homeostasis. Indeed, urinary excretion of 8-isoprostanes was significantly increased in the ezetimibe group compared with the control, and showed significant negative correlation with insulin sensitivity indices such as the Matsuda index and QUICKI in the present study (ESM Table 6). Moreover, hepatic gene expression in the ezetimibe group showed coordinated upregulation of genes involved in the immune response compared with those in the control group, suggestive of oxidative stress caused by ezetimibe treatment.

Pathway analysis of the metabolic network showed unique metabolic changes in the ezetimibe group compared with the control group. In the control group, genes involved in the CoA-biosynthesis pathway were coordinately downregulated, and those in the glycerol-3 phosphate pathway coordinately upregulated, suggesting activated triacylglycerols biosynthesis. In the ezetimibe group,

Table 6 Changes in hepatic fatty acid composition

Fatty acid	Control		p^a	Ezetimibe		p^a	p^b
	Before	After		Before	After		
C12:0 (lauric acid)	7.7±1.2	15.2±5.6	0.219	6.3±1.8	18.8±4.7	0.019	0.494
C14:0 (myristic acid)	19.9±2.5	33.0±10.1	0.228	17.6±2.2	56.6±13.0	0.014	0.148
C16:0 (palmitic acid)	185.9±23.8	303.9±118.2	0.334	169.7±22.9	583.9±176.8	0.042	0.202
C16:1n-7 (palmitoleic acid)	24.2±4.5	37.3±13.4	0.362	22.3±4.3	51.9±13.2	0.031	0.368
C17:0 (margaric acid)	4.6±0.7	3.5±0.1	0.400	5.3±0.8	16.0±4.1	0.024	0.025
C18:0 (stearic acid)	45.9±4.4	54.4±8.9	0.283	56.0±7.1	125.1±30.2	0.017	0.042
C18:1n-9 (oleic acid)	166.4±25.1	250.2±91.6	0.367	173.9±30.6	381.9±84.3	0.017	0.288
C18:2n-6 (linoleic acid)	80.4±12.3	87.9±22.5	0.556	73.9±8.5	147.3±36.1	0.035	0.066
C18:3n-6 (γ-linolenic acid)	ND	ND		ND	ND		
C18:3n-3 (α-linolenic acid)	0.6±0.4	0.0±0.0	0.171	0.6±0.4	0.0±0.0	0.178	0.981
C20:0n-6 (arachidic acid)	ND	ND		ND	ND		
C20:1n-9 (eicosenoic acid)	5.5±1.1	4.7±1.9	0.639	5.7±1.0	13.1±4.8	0.170	0.168
C20:2n-6 (eicosadienoic acid)	ND	ND		ND	ND		
C20:3n-6 (dihomo-γ-linolenic acid)	ND	ND		ND	ND		
C20:3n-9 (eicosatrienoic acid)	ND	ND		ND	ND		
C20:4n-6 (arachidonic acid)	ND	ND		ND	ND		
C20:5n-3 (eicosapentaenoic acid)	ND	ND		ND	ND		
C22:0 (behenic acid)	ND	ND		ND	ND		
C22:1n-9 (erucic acid)	14.2±2.5	11.7±2.7	0.474	16.2±2.4	19.2±1.0	0.664	0.468
C22:2n-6 (docosadienoic acid)	2.8±1.0	1.8±1.0	0.433	22.3±0.7	62.3±2.9	0.176	0.152
C22:4n-6 (docosatetraenoic acid)	ND	ND		ND	ND		
C22:5n-3 (docosapentaenoic acid)	ND	ND		ND	ND		
C22:6n-3 (docosahexaenoic acid)	13.6±3.5	7.8±3.3	0.232	14.2±3.7	48.7±19.9	0.109	0.097
C24:1 (nervonic acid)	ND	ND		ND	ND		

The data are expressed as 10^{-4} mg/mg liver, means ± SE

[a] p value for the intragroup comparison (baseline vs 6 month)

[b] p value for the intergroup comparison (changes from baseline between groups)

ND, not determined

genes involved in the L-carnitine pathway, including *CPT1A,* were coordinately downregulated. A decreased L-carnitine pathway could be associated with reduced β-oxidation of palmitic acids in mitochondria, resulting in an increase in long-chain fatty acids (lauric, myristic, palmitic, palmitoleic, margaric, stearic, oleic and linoleic acids). Unbalanced fatty acid composition could induce oxidative stress and lead to insulin resistance in the ezetimibe group. In addition, genes involved in the cholesterol and NEFA biosynthesis, including *SREBF2*, were coordinately upregulated in the ezetimibe group (Table 3), probably as a result of deceased absorption of exogenous cholesterol. Upregulation of *SREBF2* potentially represses the expression of hepatocyte nuclear factor 4, which is required for *CPT1* transcription [35]. Moreover, recent reports have demonstrated that microRNA (miR)-33, encoded by an intron of *Srebp2* [36], inhibits translation of transcripts involved in fatty acid β-oxidation, including *CPT1* [37]. miR-33 is also implicated in decreased insulin signalling by reducing insulin receptor substrate-2 [38, 39]. Hepatic gene expression profiles may, to some extent, explain hepatic fatty acid composition and impaired glycaemic control in the ezetimibe group. These novel SREBP-2-mediated pathways in the gene expression network may be relevant to a recent report that a polymorphism in the *SREBF2* predicts incidence and the severity NAFLD and the associated glucose and lipid dysmetabolism [15]. These unique hypotheses should be confirmed in future in vitro and in vivo studies.

Our study has some limitations. First, the number of patients is relatively small because the data and safety monitoring board recommended that the study intervention and enrolment be discontinued in light of the higher proportion of adverse events in the ezetimibe group than in the control group. Second, our trial was a 6 month open-label study that resulted in subtle changes in liver pathology compared with previous reports [40]. Indeed, a 6 month duration may be too short a period to expect improvement of fibrosis, which is a slowly

progressive process [40]. Third, the average serum aminotransferase levels were lower than those in previous studies [9, 10], and most of the patients had mild steatosis, fibrosis and lower NAS at baseline before ezetimibe treatment. Serum ALT levels did not decrease with ezetimibe treatment in the present study, in contrast to the significant improvement reported previously [9, 10]. And finally, secondary outcomes are always at risk of false-positive associations. Therefore, we not only presented the changes in HbA_{1c} ($p=0.001$ for ezetimibe treatment and $p=0.041$ for the intergroup difference at the end of the study), but also showed the signature of hepatic fatty acid composition and hepatic gene expression profiles that support the hypothesis that ezetimibe increases HbA_{1c} and hepatic fatty acids contents possibly through the SREBP-2–miR33 pathway. No previous studies have raised this issue, which is worth investigating. The same mechanism may underlie a statin-induced deterioration of glucose tolerance, which remains a serious concern. Furthermore, the SREBP-2–miR33 pathway may raise a concern for a safety issue of combination therapy with ezetimibe and statins because these agents may additively upregulate *SREBF2* expression [41]. Future large-scale, long-duration studies involving more severely affected patients are required to determine the definite efficacy and risks of ezetimibe in the treatment of NAFLD.

In conclusion, the present study represents the first randomised controlled clinical trial of the efficacy of ezetimibe on liver pathology, energy homeostasis, hepatic fatty acid composition and hepatic gene expression profiles in patients with NAFLD. The lipid profile and liver histology of cell ballooning and fibrosis were significantly improved by ezetimibe treatment. However, our findings suggest an increase in oxidative stress, insulin resistance and HbA_{1c} on treatment with ezetimibe, which should be taken into consideration in NAFLD patients.

Acknowledgements We thank M. Kawamura (Kanazawa University Graduate School of Medical Sciences) for technical assistance.

Funding This work was supported by Grants-in-Aid from the Ministry of Education, Culture, Sports, Science and Technology, Japan, and research grants from MSD (to TT and SK).

Duality of interest The authors declare that there is no duality of interest associated with this manuscript.

Contribution statement YT designed the study, recruited the patients, analysed the data and wrote the manuscript. TT designed the study, recruited the patients, interpreted the data and edited the manuscript. MH analysed the hepatic gene expression profiles. YK performed the statistical analyses. YZ analysed all the biopsies. KK, HM and TO recruited the patients and collected the clinical information. HS, KA and TY performed the liver biopsies and histological examinations. MN performed the DNA chip experiments. KY and EM analysed the hepatic fatty acid compositions. SK initiated and organised the study. All authors contributed to the acquisition, analysis and interpretation of data and the drafting and editing of the manuscript. All of the authors approved the final version of the manuscript.

References

1. Hamaguchi E, Takamura T, Sakurai M et al (2010) Histological course of nonalcoholic fatty liver disease in Japanese patients: tight glycemic control, rather than weight reduction, ameliorates liver fibrosis. Diabetes Care 33:284–286
2. Sakurai M, Takamura T, Ota T et al (2007) Liver steatosis, but not fibrosis, is associated with insulin resistance in nonalcoholic fatty liver disease. J Gastroenterol 42:312–317
3. Matsuzawa N, Takamura T, Kurita S et al (2007) Lipid-induced oxidative stress causes steatohepatitis in mice fed an atherogenic diet. Hepatology 46:1392–1403
4. Marí M, Caballero F, Colell A et al (2006) Mitochondrial free cholesterol loading sensitizes to TNF- and Fas-mediated steatohepatitis. Cell Metab 4:185–198
5. Nakamura S, Takamura T, Matsuzawa-Nagata N et al (2009) Palmitate induces insulin resistance in H4IIEC3 hepatocytes through reactive oxygen species produced by mitochondria. J Biol Chem 29: 14809–14818
6. Garcia-Calvo M, Lisnock J, Bull HG et al (2005) The target of ezetimibe is Niemann-Pick C1-like 1 (NPC1L1). Proc Natl Acad Sci U S A 102: 8132–8137
7. Muraoka T, Aoki K, Iwasaki T et al (2011) Ezetimibe decreases SREBP-1c expression in liver and reverses hepatic insulin resistance in mice fed a high-fat diet. Metabolism 60:617–628
8. Deushi M, Nomura M, Kawakami A et al (2007) Ezetimibe improves liver steatosis and insulin resistance in obese rat model of metabolic syndrome. FEBS Lett 581:5664–5670
9. Yoneda M, Fujita K, Nozaki Y et al (2010) Efficacy of ezetimibe for the treatment of non-alcoholic steatohepatitis: an open-label, pilot study. Hepatol Res 40:613–621
10. Park H, Shima T, Yamaguchi K et al (2011) Efficacy of long-term ezetimibe therapy in patients with nonalcoholic fatty liver disease. J Gastroenterol 46:101–107
11. Promrat K, Lutchman G, Uwaifo GI et al (2004) A pilot study of pioglitazone treatment for nonalcoholic steatohepatitis. Hepatology 39:188–196
12. Matthews DR, Hosker JP, Rudenski AS et al (1985) Homeostasis model assessment: insulin resistance and beta-cell function from fasting plasma glucose and insulin concentrations in man. Diabetologia 28:412–419
13. Katz A, Nambi SS, Mather K et al (2000) Quantitative insulin sensitivity check index: a simple, accurate method for assessing insulin sensitivity in humans. J Clin Endocrinol Metab 85:2402–2410
14. Musso G, Cassader M, de Michieli F, Rosina F, Orlandi F, Gambino R (2012) Nonalcoholic steatohepatitis versus steatosis: adipose tissue insulin resistance and dysfunctional response to fat ingestion predict liver injury and altered glucose and lipoprotein metabolism. Hepatology 56:933–942
15. Musso G, Cassader M, Bo S, de Michieli F, Gambino R (2013) Sterol regulatory element-binding factor 2 (SREBF-2) predicts 7-year NAFLD incidence and severity of liver disease and lipoprotein and glucose dysmetabolism. Diabetes 62:1109–1120
16. Gastaldelli A, Cusi K, Pettiti M, Hardies J, Miyazaki Y, Berria R, Buzzigoli E, Sironi AM, Cersosimo E, Ferrannini E, Defronzo RA (2007) Relationship between hepatic/visceral fat and hepatic insulin resistance in nondiabetic and type 2 diabetic subjects. Gastroenterology 133:496–506
17. Musso G, Gambino R, Cassader M (2010) Lipoprotein metabolism mediates the association of MTP polymorphism with beta-cell dysfunction in healthy subjects and in nondiabetic normolipidemic patients with nonalcoholic steatohepatitis. J Nutr Biochem 21:834–840
18. Abdul-Ghani MA, Williams K, DeFronzo RA, Stern M (2007) What is the best predictor of future type 2 diabetes? Diabetes Care 30: 1544–1548

19. Matsuda M, DeFronzo RA (1999) Insulin sensitivity indices obtained from oral glucose tolerance testing: comparison with the euglycemic insulin clamp. Diabetes Care 22:1462–1470
20. Abdul-Ghani MA, Matsuda M, Balas B, DeFronzo RA (2007) Muscle and liver insulin resistance indexes derived from the oral glucose tolerance test. Diabetes Care 30:89–94
21. DeFronzo RA, Tobin JD, Andres R (1979) Glucose clamp technique: a method for quantifying insulin secretion and resistance. Am J Physiol 237:E214–E223
22. Nagai Y, Takamura T, Nohara E et al (1999) Acute hyperinsulinemia reduces plasma concentrations of homocysteine in healthy men. Diabetes Care 22:1004
23. Brunt EM, Janney CG, Di Bisceglie AM et al (1999) Nonalcoholic steatohepatitis: a proposal for grading and staging the histological lesions. Am J Gastroenterol 94:2467–2474
24. Kleiner DE, Brunt EM, van Natta M et al (2005) Nonalcoholic Steatohepatitis Clinical Research Network. Design and validation of a histological scoring system for nonalcoholic fatty liver disease. Hepatology 41:1313–1321
25. DeBose-Boyd RA, Ou J, Goldstein JL, Brown MS (2001) Expression of sterol regulatory element-binding protein 1c (SREBP-1c) mRNA in rat hepatoma cells requires endogenous LXR ligands. Proc Natl Acad Sci U S A 13:1477–1482
26. de Bari O, Neuschwander-Tetri BA, Liu M et al (2012) Ezetimibe: its novel effects on the prevention and the treatment of cholesterol gallstones and nonalcoholic fatty liver disease. J Lipids 2012:302847
27. Jia L, Ma Y, Rong S et al (2010) Niemann-Pick C1-Like 1 deletion in mice prevents high-fat diet-induced fatty liver by reducing lipogenesis. J Lipid Res 51:3135–3144
28. Musso G, Gambino R, Cassader M (2013) Cholesterol metabolism and the pathogenesis of non-alcoholic steatohepatitis. Prog Lipid Res 52:175–191
29. Teratani T, Tomita K, Suzuki T et al (2012) A high-cholesterol diet exacerbates liver fibrosis in mice via accumulation of free cholesterol in hepatic stellate cells. Gastroenterology 142:152–164
30. Altmann SW, Davis HR Jr, Zhu LJ et al (2004) Niemann-Pick C1 Like 1 protein is critical for intestinal cholesterol absorption. Science 303:1201–1204
31. Temel RE, Brown JM, Ma Y et al (2007) Hepatic Niemann-Pick C1-like 1 regulates biliary cholesterol concentration and is a target of ezetimibe. J Clin Invest 117:1968–1978
32. Joshi-Barve S, Barve SS, Amancherla K et al (2007) Palmitic acid induces production of proinflammatory cytokine interleukin-8 from hepatocytes. Hepatology 46:823–830
33. Pagliassotti MJ, Wei Y, Wang D (2007) Insulin protects liver cells from saturated fatty acid-induced apoptosis via inhibition of c-Jun NH2 terminal kinase activity. Endocrinology 148:3338–3345
34. Malhi H, Bronk SF, Werneburg NW, Gores GJ (2006) Free fatty acids induce JNK-dependent hepatocyte lipoapoptosis. J Biol Chem 281: 12093–12101
35. Gerin I, Clerbaux LA, Haumont O et al (2010) Expression of miR-33 from an SREBP2 intron inhibits cholesterol export and fatty acid oxidation. J Biol Chem 285:33652–33661
36. Louet JF, Hayhurst G, Gonzalez FJ et al (2002) The coactivator PGC-1 is involved in the regulation of the liver carnitine palmitoyltransferase I gene expression by cAMP in combination with HNF4 alpha and cAMP-response element-binding protein (CREB). J Biol Chem 277:37991–38000
37. Xuefen X, Hailing L, Huaixin D et al (2009) Down-regulation of hepatic HNF4_ gene expression during hyperinsulinemia via SREBPs. Mol Endocrinol 23:434–443
38. Horie T, Ono K, Horiguchi M et al (2010) MicroRNA-33 encoded by an intron of sterol regulatory element-binding protein 2 (Srebp2) regulates HDL in vivo. Proc Natl Acad Sci U S A 107:17321–17326
39. Fernández-Hernando C, Moore KJ (2011) MicroRNA modulation of cholesterol homeostasis. Arterioscler Thromb Vasc Biol 31:2378–2382
40. Musso G, Cassader M, Rosina F, Orlandi F, Gambino R (2012) Impact of current treatments on liver disease, glucose metabolism and cardiovascular risk in non-alcoholic fatty liver disease (NAFLD): a systematic review and meta-analysis of randomised trials. Diabetologia 55:885–904
41. Bennett MK, Seo YK, Datta S, Shin DJ, Osborne TF (2008) Selective binding of sterol regulatory element-binding protein isoforms and co-regulatory proteins to promoters for lipid metabolic genes in liver. J Biol Chem 6:15628–15637

HEPATOLOGY
Official Journal of the American Association for the Study of Liver Diseases

Hepatic Interferon-Stimulated Genes Are Differentially Regulated in the Liver of Chronic Hepatitis C Patients With Different Interleukin-28B Genotypes

Masao Honda,[1,2] Takayoshi Shirasaki,[2] Tetsuro Shimakami,[1] Akito Sakai,[1] Rika Horii,[1] Kuniaki Arai,[1] Tatsuya Yamashita,[1] Yoshio Sakai,[1] Taro Yamashita,[1] Hikari Okada,[1] Kazuhisa Murai,[1] Mikiko Nakamura,[2] Eishiro Mizukoshi,[1] and Shuichi Kaneko[1]

Pretreatment up-regulation of hepatic interferon (IFN)-stimulated genes (ISGs) has a stronger association with the treatment-resistant interleukin (IL)28B minor genotype (MI; TG/GG at rs8099917) than with the treatment-sensitive IL28B major genotype (MA; TT at rs8099917). We compared the expression of ISGs in the liver and blood of 146 patients with chronic hepatitis C who received pegylated IFN and ribavirin combination therapy. Gene expression profiles in the liver and blood of 85 patients were analyzed using an Affymetrix GeneChip (Affymetrix, Santa Clara, CA). ISG expression was correlated between the liver and blood of the MA patients, whereas no correlation was observed in the MI patients. This loss of correlation was the result of the impaired infiltration of immune cells into the liver lobules of MI patients, as demonstrated by regional gene expression analysis in liver lobules and portal areas using laser capture microdissection and immunohistochemical staining. Despite having lower levels of immune cells, hepatic ISGs were up-regulated in the liver of MI patients and they were found to be regulated by multiple factors, namely, IL28A/B, IFN-λ4, and wingless-related MMTV integration site 5A (WNT5A). Interestingly, WNT5A induced the expression of ISGs, but also increased hepatitis C virus replication by inducing the expression of the stress granule protein, GTPase-activating protein (SH3 domain)-binding protein 1 (G3BP1), in the Huh-7 cell line. In the liver, the expression of WNT5A and its receptor, frizzled family receptor 5, was significantly correlated with G3BP1. *Conclusions:* Immune cells were lost and induced the expression of other inflammatory mediators, such as WNT5A, in the liver of IL28B minor genotype patients. This might be related to the high level of hepatic ISG expression in these patients and the treatment-resistant phenotype of the IL28B minor genotype. (HEPATOLOGY 2014;00:000-000)

Interferon (IFN) and ribavirin (RBV) combination therapy has been a popular modality for treating patients with chronic hepatitis C (CHC); however, ~50% of patients usually relapse, particularly those with hepatitis C virus (HCV) genotype 1b and a high viral load.[1] The recently developed direct-acting antiviral drug, telaprevir, combined with pegylated (Peg)-IFN plus RBV, significantly improved sustained virologic response (SVR) rates; however, the SVR rate was not satisfactory (29%-33%) in patients who had no

Abbreviations: ALT, alanine aminotransferase; AST, aspartate aminotransferase; CCL, CC chemokine ligand; CHC, chronic hepatitis C; CLLs, cells in liver lobules; CPAs, cells in portal areas; CXCL10/IP-10, chemokine (C-X-C motif) ligand 10/interferon-gamma-induced protein 10; CXCR3, chemokine (C-X-C motif) receptor 3; DCs, dendritic cells; DVL, disheveled; FZD5, frizzled family receptor 5; G3BP1, GTPase-activating protein (SH3 domain)-binding protein 1; GGT, gamma-glutamyl transpeptidase; HCV, hepatitis C virus; IFI44, interferon-induced protein 44; IFIT1, interferon-induced protein with tetratricopeptide repeats 1; IFN, interferon; IHC, immunohistochemical; IL, interleukin; ISGs, interferon-stimulated genes; JFH-1, Japanese fulminant hepatitis type 1; LCM, laser capture microdissection; MA, major genotype; MAd, major genotype, down-regulated; MAu, major genotype, up-regulated; MI, minor genotype; Mx, myxovirus (influenza virus) resistance; NK, natural killer; OAS2, 2′-5′-oligoadenylate synthetase 2; PALT, portal-tract-associated lymphoid tissue; Peg_IFN, pegylated IFN; RBV, ribavirin; RTD-PCR, real-time detection polymerase chain reaction; SG, stress granule; siRNA, small interfering RNA; SVR, sustained virologic response; WNT5A, wingless-related MMTV integration site 5A.

From the [1]Department of Gastroenterology, Kanazawa University Graduate School of Medicine, Kanazawa, Japan; and [2]Department of Advanced Medical Technology, Kanazawa University Graduate School of Health Medicine, Kanazawa, Japan.

Received May 31, 2013; accepted September 30, 2013.

response to previous therapy.[2] Therefore, IFN responsiveness is still an essential clinical determinant for treatment response to triple (Peg-IFN+RBV+DAA) therapy.

A recent landmark genome-wide association study identified a polymorphism in the interleukin (IL)28B, IFN-λ3) gene that was associated with either a sensitive (major genotype; MA) or resistant (minor genotype; MI) treatment response to Peg-IFN and RBV combination therapy and was characterized by either up- (-u) or down-regulation (-d) of interferon-stimulated genes (ISGs).[3-5] However, the underlying mechanism for the association of this polymorphism and treatment response has not been clarified. Previously, we showed that up-regulation of the pretreatment expression of hepatic ISGs was associated with an unfavorable treatment outcome and was closely related to the treatment-resistant IL28B genotype (TG or GG at rs8099917).[6] It could be speculated that the pretreatment activation of ISGs would repress additional induction of ISGs after treatment with exogenous IFN. However, it is unknown how hepatic ISGs are up-regulated in treatment-resistant CHC patients and why patients with high levels of ISG expression cannot eliminate HCV. Therefore, other mechanisms should be involved in the unfavorable treatment outcome of patients with the treatment-resistant IL28B genotype.

In the present study, we performed gene expression profiling in the liver and blood and compared the expression of ISGs between them. Furthermore, ISG expression in liver lobules and portal areas was analyzed separately using a laser capture microdissection (LCM) method. Finally, we identified an immune factor that is up-regulated in patients with the treatment-resistant IL28B genotype and mediates favorable signaling for HCV replication.

Materials and Methods

Patients. We analyzed 168 patients with CHC who had received Peg-IFN-α2b (Schering-Plough K.K., Tokyo, Japan) and RBV combination therapy for 48 weeks at the Graduate School of Medicine, Kanazawa University Hospital, Japan and its related hospitals, as reported previously (Table 1 and Supporting Table 1).[6]

Preparation of Liver Tissue and Blood Samples. A liver biopsy was performed on samples from 168 patients, and blood samples were obtained from 146 of these patients before starting therapy (Table 1 and Supporting Table 1). Detailed procedures are described in the Supporting Materials and Methods.

Affymetrix GeneChip Analysis. Liver tissue samples from 91 patients and blood samples from 85 patients were analyzed using an Affymetrix GeneChip (Affymetrix, Santa Clara, CA). LCM analysis was performed in 5 MAu, MAd, and MI patients. Affymetrix GeneChip analysis and LCM were performed, as described previously.[6,7] Detailed procedures are described in the Supporting Materials and Methods.

Hierarchical Clustering and Pathway Analysis of GeneChip Data. GeneChip data analysis was performed using BRB-Array Tools (http://linus.nci.nih.gov/BRB-ArrayTools.htm), as described previously.[7] Pathway analysis was performed using MetaCore (Thomson Reuters, New York, NY). Detailed procedures are described in the Supporting Materials and Methods.

Quantitative Real-Time Detection Polymerase Chain Reaction, Cell Lines, Cell Migration Assay, Vector Preparation, HCV Replication Analysis, and Statistical Analysis. These procedures are described in detail in the Supplemental Material and Methods.

Results

Differential ISG Expression in Liver and Blood of Patients With Different IL28B Genotypes. Previously, we showed that pretreatment up-regulation of hepatic ISGs was associated with an unfavorable treatment outcome and was closely related to the treatment-resistant IL28B MI (TG or GG at rs8099917).[6] To examine whether expression of hepatic ISGs would reflect the expression of blood ISGs, we compared ISG expression between the liver and blood. We utilized three ISGs (interferon-induced protein 44 [IFI44], interferon-induced protein with

Address reprint requests to: Shuichi Kaneko, M.D., Ph.D., Department of Gastroenterology, Graduate School of Medicine, Kanazawa University, Takara-Machi 13-1, Kanazawa 920-8641, Japan. E-mail: skaneko@m-kanazawa.jp; fax: +81-76-234-4250.

View this article online at wileyonlinelibrary.com.

DOI 10.1002/hep.26788

Potential conflict of interest: Nothing to report.

Additional Supporting Information may be found in the online version of this article.

Table 1. Clinical Characteristics of 146 Patients Whose Liver and Blood Samples Were Analyzed by RT-PCR

	Major (MA)				Minor (MI)		
Clinical Category	**Major ISG Up (MAu)**		**Major ISG Down (MAd)**				***P* Value**
No. of patients	n = 42		n = 68		n = 36		NA
Age and sex							
Age (years)	55	(30-72)	56	(31-72)	55	(30-73)	NS
Sex (M vs. F)	27 vs. 15		34 vs. 34		19 vs. 17		NS
Treatment responses							
SVR/TR/NR	24/12/6		30/33/6		6/7/23*		MAu vs. MI < 0.0001, MAd vs. MI < 0.0001
IL28B genotype (TT vs. TG+GG)	TT		TT		TG/GG (31/5)		NA
Liver factors							
F stage (1/2/3/4)	14/13/11/4		30/20/11/7		14/8/10/4		NS
A grade (A0-1 vs. A2-3)	16 vs. 26		37 vs. 31		20 vs. 16		NS
ISGs (Mx1, IFI44, IFIT1)	3.83*	(2.14-9.48)	1.30*	(0.36-2.08)	5.52*	(0.86-17.3)	MAu vs. MAd < 0.0001, MAu vs. MI < 0.0001, MAd vs. MI < 0.0001
IL28A/B	41.3*	(4-151)	11.7*	(1-53)	22.7*	(3-93)	MAu vs. MAd < 0.0001, MAu vs. MI = 0.0004, MAd vs. MI = 0.031
Blood factors							
ISGs (Mx1, IFI44, IFIT1)	11.1*	(2.78-24.9)	4.76	(0.41-20.6)	5.64	(0.71-2.8)	MAu vs. MAd < 0.0001, MAu vs. MI < 0.0001
IL28A/B	1.6	(0.1-7.7)	1.3	(0.2-6.4)	1.3	(0.3-3.6)	NS
Laboratory parameters							
HCV-RNA (KIU/mL)	2,430	(160-5,000)	2,692	(140-5,000)	1,854*	(126-5,000)	MAd vs. MI = 0.017
BMI (kg/m2)	24	(18.7-31.9)	24	(16.3-34.7)	22.8	(19.1-30.5)	NS
AST (IU/L)	86*	(22-258)	54	(18-192)	64	(21-178)	MAu vs. MAd = 0.0008
ALT (IU/L)	112*	(17-376)	75	(16-345)	79	(18-236)	MAu vs. MAd = 0.023
γ-GTP (IU/L)	99*	(21-392)	47	(4-367)	74	(20-298)	MAu vs. MAd = 0.0003
WBC (/mm3)	4,761	(2,100-8,100)	4,982	(2,800-9,100)	4,823	(2,500-8,200)	NS
Hb (g/dL)	14.1	(11.4-16.7)	14.1	(9.3-16.9)	13.9	(11.2-16.4)	NS
PLT (× 104/mm3)	15.2	(9.2-27.8)	16.8	(7-39.4)	16.3	(9-27.8)	NS
TG (mg/dL)	112	(42-248)	102	(42-260)	136*	(30-323)	MAd vs. MI = 0.02
T-Chol (mg/dL)	162	(90-221)	169	(107-229)	167	(81-237)	NS
LDL-Chol (mg/dL)	77	(36-123)	83*	(42-134)	72	(29-107)	MAd vs. MI = 0.04
HDL-Chol (mg/dL)	40	(18-67)	43	(27-71)	47*	(27-82)	NS
Viral factors							
ISDR mutations ≦ 1 vs. ≧ 2	23 vs. 19*		51 vs. 17		26 vs. 10		MAu vs. MAd = 0.02
Core aa 70 (wild-type vs. mutant)	24 vs. 18		42 vs. 22		16 vs. 20*		MAd vs. MI = 0.02

*$P < 0.05$.

Abbreviations: BMI, body mass index; ALT, alanine aminotransferase; WBC, leukocytes; Hb, hemoglobin; PLT, platelets; TG, triglycerides; T-chol, total cholesterol; LDL-chol, low density lipoprotein cholesterol; HDL-chol, high density lipoprotein cholesterol; NA, not applicable; NS, not significant.

tetratricopeptide repeats 1 [IFIT1], and myxovirus (influenza virus) resistance [Mx1]) with a high dynamic range, comparable relative expression, and good predictive performance.[6] Mean values of the three ISGs detected by real-time detection polymerase chain reaction (RTD-PCR) in 168 liver tissue samples (Supporting Table 1) showed a significant up-regulation of their expression in nonresponder or treatment-resistant IL28B MI (TG/GG; rs8099917) patients, compared to responder (SVR+TR) or treatment-sensitive IL28B MA (TT; rs8099917) patients, as reported previously (Fig. 1A and Supporting Fig. 1A).[6] However, ISG expression in 146 blood samples (Table 1) showed no difference between responders and nonresponders or the IL28B major and minor genotypes (Fig. 1B and Supporting Fig. 1B). To explore these findings further, gene expression profiling using Affymetrix GeneChips was performed on liver and blood samples from 85 patients (Supporting Tables 2 and 3), and the expression of 37 representative ISGs[6] was compared (Fig. 1C-E). MA patients were divided into two groups according to their ISG expression pattern in the liver: MAu and MAd. MI patients expressed ISGs at a higher level than MAu patients. Interestingly, ISG expression in MA patients showed a similar expression pattern in liver and blood, and ISGs were up-regulated in MAu patients and down-regulated in the MAd patients. However, MI patients showed a different ISG expression pattern in liver and blood, where ISGs were up-regulated in the liver, but down-regulated in the blood (Fig. 1C). The correlation of the mean values of the three ISGs (IFI44, IFIT1, and Mx1) between liver and blood from 146 patients demonstrated a significant correlation between values in MA patients (Fig. 1D), whereas no correlation was observed in MI patients (Fig. 1E). Interestingly, ISG expression correlated significantly between liver and blood of responders, but not of nonresponders, in MA and MI patients (Supporting Fig. 1C-F). These results indicate that the correlation of ISG expression in the liver and blood is an important predictor of treatment response.

Clinical Characteristics of IL28B MA Patients With Up- and Down-Regulated ISGs and IL28B MI Patients. From the expression pattern of ISGs and mean values of the three ISGs (IFI44, IFIT1, and Mx1), we could use receiver operating characteristic curve analysis to set a threshold of 2.1-fold to differentiate MAu and MAd patients. Following this criterion, 42 MAu, 68 MAd, and 36 MI patients (total, 146) were grouped (Table 1). Hepatic ISG expression was highest in MI patients, whereas blood ISG expression was highest in MAu patients. Conversely, hepatic IL28A/B (IFN-λ2/3) expression was highest in MAu patients, whereas blood IL28A/B expression showed no difference among the three groups. Serum alanine aminotransferase (ALT), aspartate aminotransferase (AST), and gamma-glutamyl transpeptidase (GGT) levels were significantly higher in MAu patients than in MAd patients. Interestingly, serum ALT levels were significantly correlated with ISG expression in MA patients, but not in MI patients (Supporting Fig. 2E,F).

Gene expression profiling in peripheral immune cells showed the presence of active inflammation in MAu patients, whereas the inactive or remissive phase of inflammation was observed in MAd patients. In contrast, monophasic and intermediate inflammation existed in MI patients (Supporting Fig. 3).

Reduced Number of Immune Cells in the Liver Lobules of IL28B MI Patients. To examine the discordant expression of ISGs in liver and blood of MI patients, we performed LCM to collect cells in liver lobules (CLLs) and cells in portal areas (CPAs) separately from each of five liver biopsied samples from MAu, MAd, and MI patients (Fig. 2A). Interestingly, the ISG expression pattern in CLLs from MA patients was similar to that of CPAs, and ISGs were up-regulated in MAu patients and down-regulated in MAd patients. ISG expression in CLLs from the MI patients was different to that in CPAs, and ISGs were up-regulated in CLLs, but down-regulated in CPAs (Fig. 2A). We hypothesized that the discordance of ISG expression between CLLs and CPAs in MI patients might be the result of the lower number of immune cells that infiltrated the liver lobules of these patients. To prove this hypothesis, immunohistochemical (IHC) staining was performed (Fig. 2B). IHC staining showed that IFI44 was strongly expressed in the cytoplasm and nucleus of CLLs from MI patients, whereas it was intermediately expressed in MAu patients and weakly expressed in MAd patients. Interestingly, IFI44 was strongly expressed in CPAs of MAu patients and weakly expressed in CPAs of MAd patients, showing a correlation between expression in CLLs and CPAs of MA patients, whereas ILI44 expression was relatively weak in CPAs, compared with CLLs, in MI patients (Fig. 2B). In the same section of the specimens, there were less CD163-positive monocytes and macrophages in MI patients than in MAu and MAd patients. Similarly, there were fewer CD8-positive T cells in MI patients than in MAu and MAd patients (Fig. 2B). Semiquantitative evaluation of CD163- and CD8-positive lymphocytes in liver lobules showed a significantly lower number of cells in

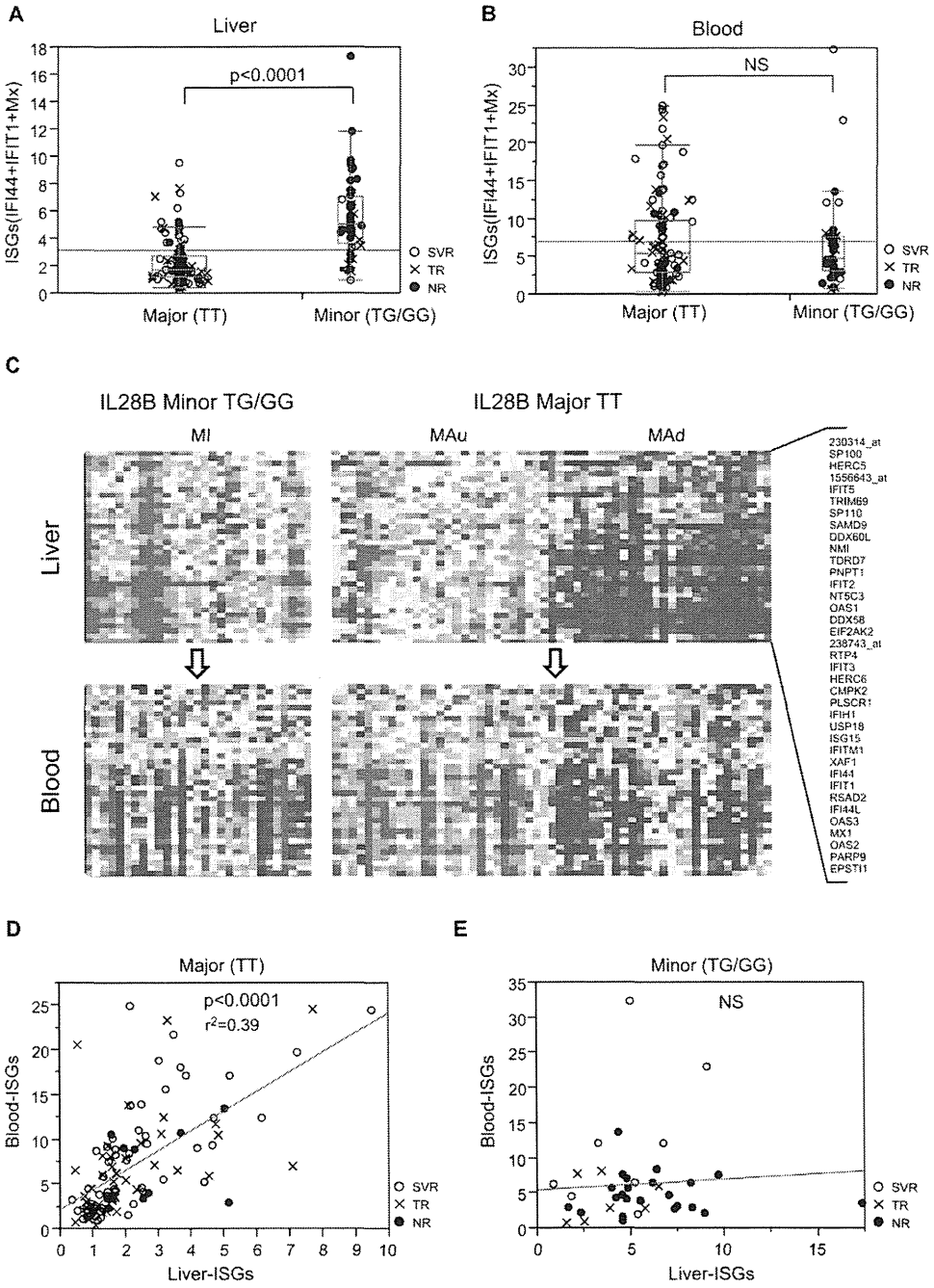

Fig. 1. Comparison of ISG expression in liver and blood of patients with different IL28B genotypes. (A and B) RTD-PCR results of mean ISG expression (IFI44-IFIT1+Mx1) in liver (A) and blood (B) of IL28B major (MAu/Mad) and minor (MI) genotype patients. (C) One-way hierarchical clustering analysis of 85 patients using 37 representative ISGs derived from liver (upper) and blood (lower). (D and E) Correlation of mean ISG expression (IFI44-IFIT1+Mx1) in liver and blood of IL28B major (MA; D) and minor (MI; E) genotype patients.

MI patients than in MAu and MAd patients (Supporting Fig. 4A,B). To support these findings, we examined the expression of 24 surface markers of immune cells in CLL, including dendritic cells (DCs), natural killer (NK) cells, macrophages, T cells, B cells, and granulocytes (Supporting Fig. 5A). The expression of immune cell-surface markers was repressed in MI patients, compared to MAu and MAd patients. Furthermore, whole-liver expression profiling in 85 patients showed the reduced expression of these surface markers in MI patients, compared to MAu and MAd patients (Supporting Fig. 5B). These results indicated that fewer immune cells had infiltrated the liver lobules of MI patients.

In addition to these findings, various chemokines, such as CC chemokine ligand (CCL)19, CCL21, CCL5, and chemokine (C-X-C motif) ligand (CXCL)13, which are important regulators for the recruitment of DCs, NK cells, T cells, and B cells in the liver, were significantly down-regulated in MI patients, compared to MAd and MAu patients (Supporting Fig. 4C-F).

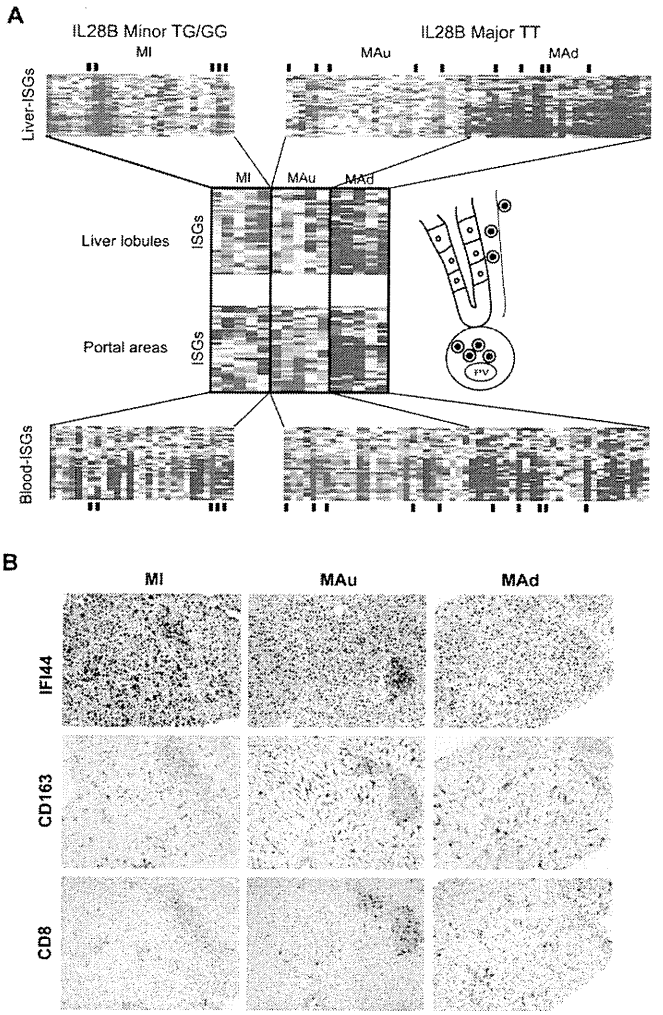

Fig. 2. LCM and IHC staining of biopsied liver specimens. (A) Comparison of the ISG expression pattern of whole liver (upper), CLLs (upper middle), CPAs (lower middle), and blood (bottom). CLLs and CPAs were obtained from 5 MI, MAu, and MAd patients, who are indicated by small black bars. (B) IHC staining of IFI44, CD163, and CD8 in MI, MAu, and MAd patients.

Hepatic ISG Expression Is Significantly Correlated With IL28A/B, but not IFN-α or IFN-β. The lower number of immune cells in the liver lobules of MI patients implies that reduced levels of IFN are produced from DCs, macrophages, and so on. These findings prompted us to examine the relationship between hepatic ISGs and IFN-α, IFN-β, IL29/IFN-λ1, and IL28A/B in CHC patients. Hepatic ISG expression was significantly correlated with IL28A/B, but not IFN-β (Fig. 3A-C) or IFN-α (data not shown) in MAu, MAd, and MI patients. Expression of IL29 was correlated with hepatic ISG expression only in MAu patients. These results indicate that hepatic ISGs would be mainly induced by IL28A/B in CHC patients. Interestingly, the correlation between hepatic ISGs and IL28A/B was strongest in MA patients ($P < 0.0001$ in MAu; $P = 0.0006$ in MAd), whereas rather a weak correlation was observed in MI patients ($P = 0.015$). Moreover, the ratio of hepatic ISGs to IL28A/B was larger in MI patients than in MA patients (S = 0.061 in MI; S = 0.028 in MAu; S = 0.020 in MAd), suggesting the presence of additional factors that can induce expression of ISGs in MI patients. Therefore, we evaluated the expression of the recently discovered IFN-λ4 in MI patients. Interestingly, there was a significant correlation between hepatic ISG and IFN-λ4 expression ($P = 0.0003$; Fig. 3C).

Wingless-Related MMTV Integration Site 5A and Its Receptor, Frizzled Receptor 5, Are Significantly Up-Regulated in the Liver of Patients With the IL28B MI. IFN-λ4 is a promising factor to induce ISG expression in MI patients,[8] and the functional relevance of IFN-λ4 for the pathogenesis of CHC is under investigation. We searched for other factors that could induce ISG expression in MI patients. A closer observation of gene expression profiling in CLLs obtained by LCM demonstrated that WNT signaling was specifically up-regulated in MI patients

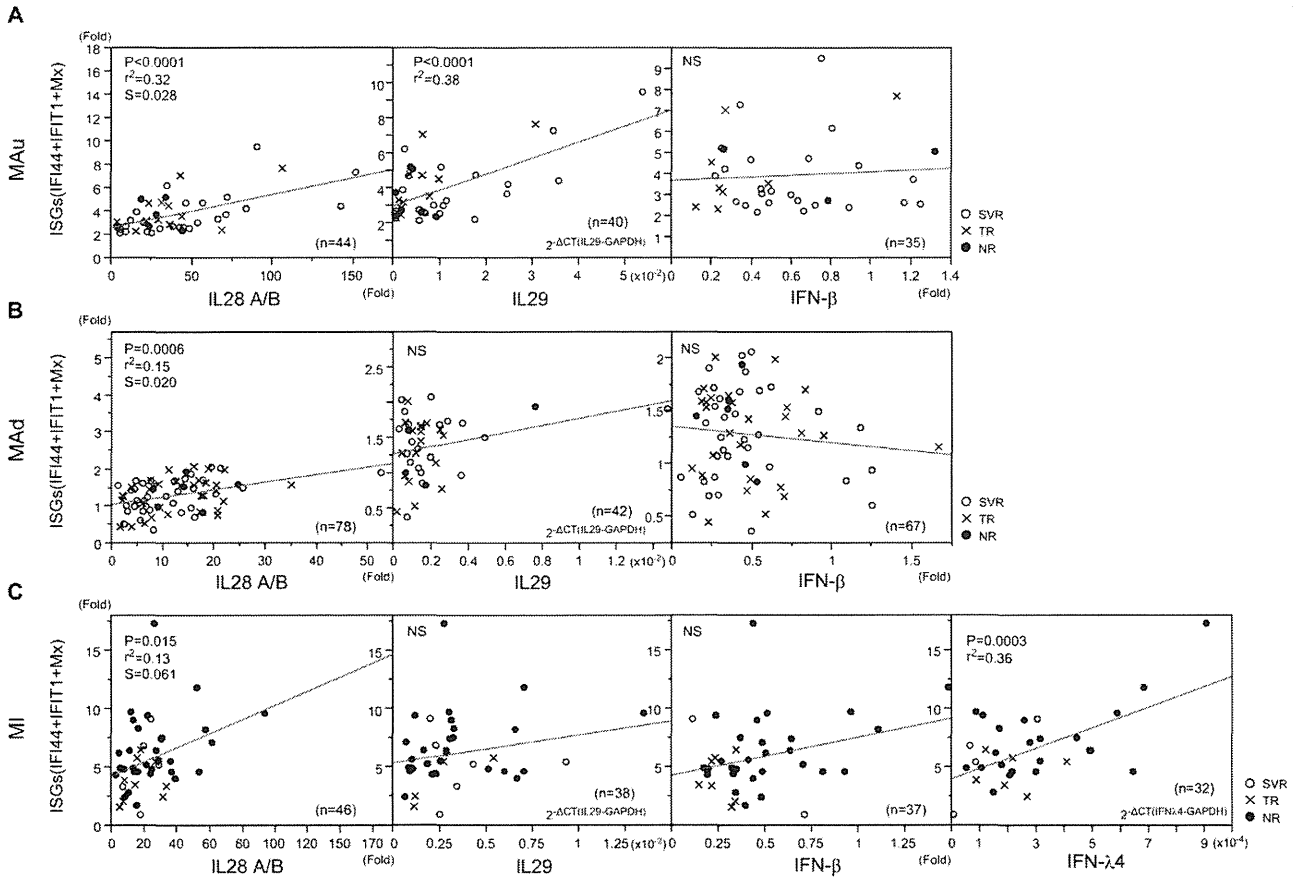

Fig. 3. Correlation analysis of hepatic ISGs and IL28A/B, IL29, IFN-β, and IFN-λ4. Correlation of mean ISG (IFI44+IFIT1+Mx1) and IL28A/B, IL29, IFN-β, and IFN-λ4 expression was evaluated in MAu (A), MAd (B), and MI (C) patients. [Color figure can be viewed in the online issue, which is available at wileyonlinelibrary.com.]

(Supporting Fig. 6). Further observation enabled us to identify that the WNT ligand, wingless-related MMTV integration site 5A (WNT5A), and its receptor, frizzled receptor 5 (FZD5), were up-regulated in MI patients. RTD-PCR results on 168 liver-biopsied samples confirmed the significant up-regulation of WNT5A and FZD5 in MI patients, compared to MAu and MAd patients (Fig. 4A,B). Interestingly, WNT5A expression was negatively correlated with chemokine expression (Supporting Fig. 7). IHC staining showed up-regulation of FZD5 in liver lobules of MI patients, but not in MAu or MAd patients (Fig. 4C). WNT5A expression was significantly correlated with hepatic ISG expression in MI and MAd patients (Fig. 4D). Interestingly, we found a weak, but significant, correlation between WNT5A and IFN-λ4 expression in MI patients (Fig. 4E).

WNT5A Induces ISG Expression, but Stimulates HCV Replication in Huh-7 Cells. To examine the functional relevance of up-regulated expression of WNT5A in MI patients, we first evaluated expression levels of WNT5A and ISGs (2′-5′-oligoadenylate synthetase 2 [OAS2], Mx1, IFI44, and IFIT1) in two immortalized human hepatocyte cell lines, THLE-5b and TTNT cells (Supporting Materials and Methods), and one human hepatoma cell line, Huh-7 cells (Supporting Fig. 8A,B). WNT5A was moderately expressed in THLE-5b and TTNT cells, whereas its expression in Huh-7 cells was minimal. Interestingly, ISG expression in these cells correlated well with expression of WNT5A (Supporting Fig. 8B). Small interfering RNA (siRNA) to WNT5A efficiently repressed WNT5A expression to ~20% of the control in THLE-5b cells, and in this condition, ISG expression was significantly decreased to 30%-50% of the control (Supporting Fig. 8C). Conversely, transduction of WNT5A using a lentivirus expression system in Huh-7 cells significantly increased OAS2 expression (Supporting Fig. 8D), as well as Mx1 and IFIT1 expression (data not shown), in the presence and absence of HCV infection. Surprisingly, HCV replication, as determined using Gaussia luciferase activity, increased in WNT5A-transduced cells (Supporting Fig. 8E). Furthermore, WNT5A-transduced cells supported more HCV replication than

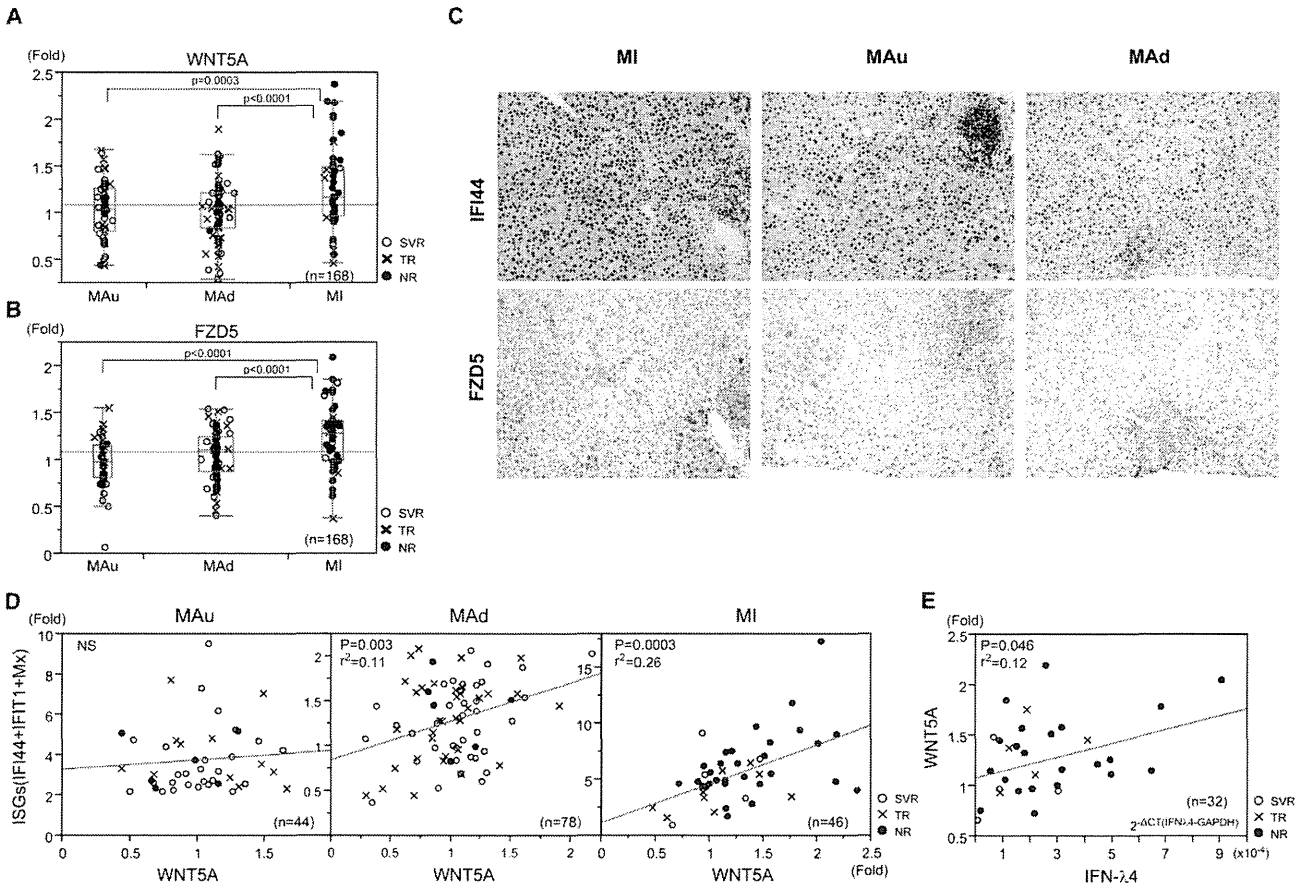

Fig. 4. WNT5A and FZD5 are up-regulated in IL28B MI patients. (A) RTD-PCR results of WNT5A expression in liver of MAu, MAd, and MI patients. (B) RTD-PCR results of FZD5 expression in liver of MAu, MAd, and MI patients. (C) IHC staining of IFI44 and FZD5 expression in liver of MAu, MAd, and MI patients. (D) Correlation of mean ISG (IFI44+IFIT1+Mx1) and WNT5A expression in liver of MAu, MAd, and MI patients. (E) Correlation of WNT5A and IFN-λ4 expression in liver of MI patients.

nontransduced cells under IFN treatment (Supporting Fig. 8F).

WNT5A-FZD5 Signaling Induces the Expression of the Stress Granule Protein, GTPase-Activating Protein (SH3 Domain)-Binding Protein 1, Which Supports HCV Replication. These findings were further confirmed by using Huh-7 cells that were continuously infected with Japanese fulminant hepatitis type 1 (JFH-1; Huh7-JFH1), which is a genotype 2a HCV isolate.[9] Interestingly, expression of WNT5A in Huh7-JFH1 cells was significantly up-regulated, compared with uninfected Huh-7 cells, and showed an equivalent expression level with THLE-5b cells (Fig. 5A). siRNA to WNT5A efficiently repressed WNT5A expression to ~20% of the control, and in this condition, ISG expression (IFI44 was not expressed in Huh-7 cells), HCV RNA, and infectivity were repressed to 25%-65%, 60%, and 40% of the control, respectively (Fig. 5B and Supporting Fig. 9A). Interestingly, CXCL13 expression was significantly increased in this condition. We evaluated the expression of GTPase-activating protein (SH3 domain)-binding protein 1 (G3BP1), a recently recognized stress granule (SG) protein that supports HCV infection and replication.[10] Expression of G3BP1 was repressed to 60% of the control by knocking down WNT5A. Conversely, overexpression of WNT5A in Huh7-JFH1 cells significantly decreased CXCL13 expression and increased HCV RNA, infectivity, and G3BP1 expression (Fig. 5C and Supporting Fig. 9B). A recent report demonstrated that G3BP1 is a disheveled (DVL)-associated protein that regulates WNT signaling downstream of the FZD receptor.[11] Knocking down FZD5 in Huh7-JFH1 cells significantly reduced the expression of DVL1-3, G3BP1, Mx1, and IFIT1 as well as HCV infectivity (Supporting Fig. 9C,D). Interestingly, G3BP1 expression was significantly up-regulated in liver of MI patients (Fig. 5D). Furthermore, G3BP1 expression was significantly correlated with WNT5A expression in liver of the CHC patients (Fig. 5E). More dramatically, a strong correlation was observed between expression of FZD5 and G3BP1 in liver of CHC patients (Fig. 5F).

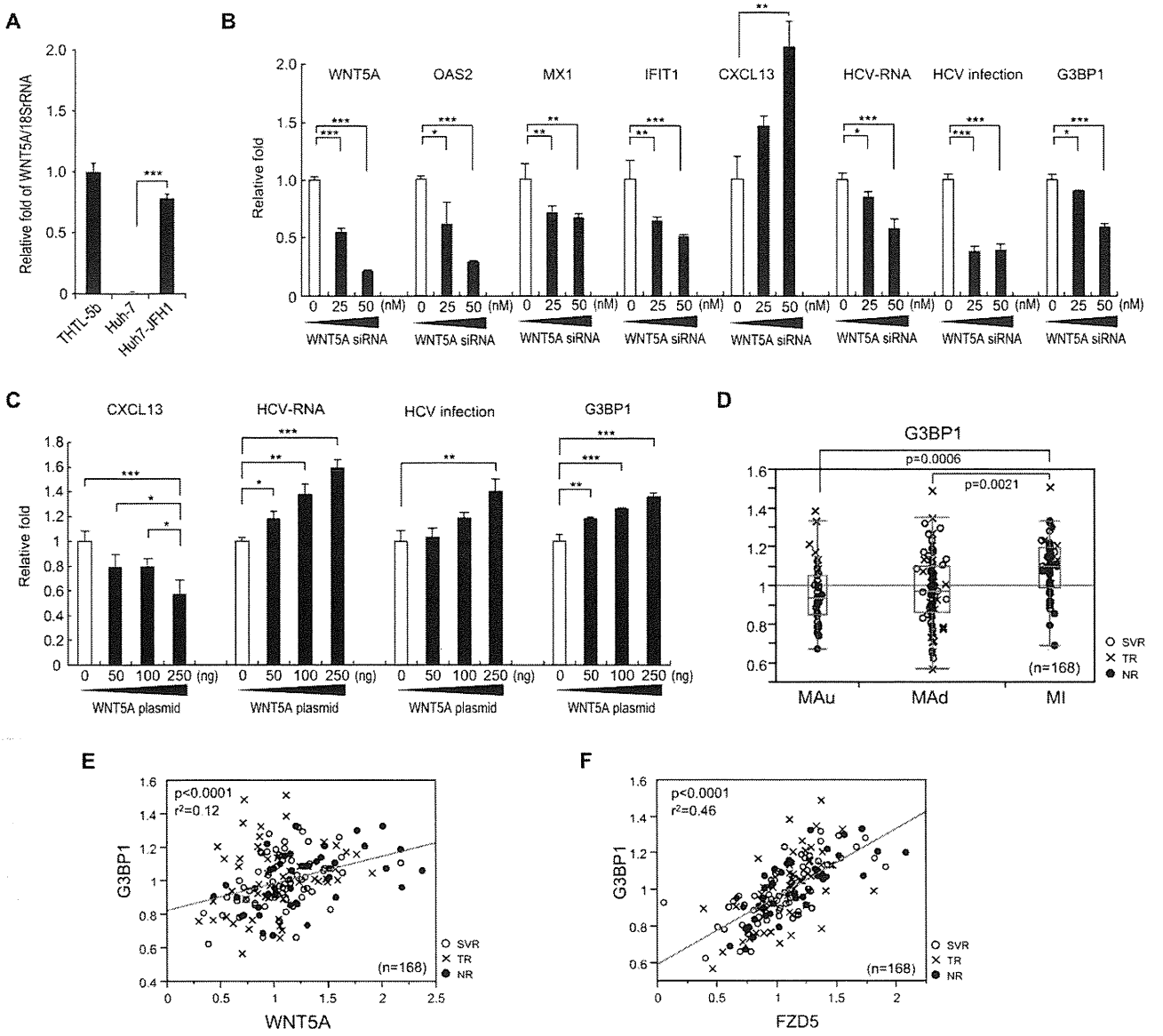

Fig. 5. Relationship between WNT5A and FZD5 signaling and the SG protein, G3BP1. (A) WNT5A expression in THLE-5b, Huh-7, and Huh7-JFH1 cells. (B) Knocking down WNT5A and changes of OAS2, Mx1, IFIT1, CXCL13, and G3BP1 expression, HCV RNA, and infectivity in Huh7-JFH1 cells. (C) Overexpression of WNT5A after transfection with pCMV-WNT5A and decrease in CXCL13 expression and increase in HCV RNA, infectivity, and G3BP1 expression. (A-C) Experiments were performed in duplicate and repeated three times (n = 6). Values are the means ± standard error. $*P < 0.05$; $**P < 0.01$; $***P < 0.005$. (D) RTD-PCR results for G3BP1 expression in liver of MAu, MAd, and MI patients. (E) Correlation of WNT5A and G3BP1 expression in the liver. (F) Correlation of FZD5 and G3BP1 expression in the liver. [Color figure can be viewed in the online issue, which is available at wileyonlinelibrary.com.]

Discussion

The underlying mechanism for the association of the IL28B genotype with treatment responses to IFN-based therapy for HCV has not yet been clarified. We and others have shown that pretreatment up-regulation of hepatic ISGs was associated with an unfavorable treatment outcome[7,12,13] and was closely related to treatment-resistant MI IL28B, compared with treatment-sensitive MA IL28B.[6]

By comparing ISG expression in liver and blood, we found that their expression was correlated in MA patients, but not in MI patients. LCM analysis of ISG expression in CLLs and CPAs showed the loss of the correlation between CLLs and CPAs in MI patients (Fig. 2A). This might be the result of the impaired migration of immune cells into liver lobules that was demonstrated by decreased expression of immune cell-surface markers in CLLs by LCM (Supporting Fig. 5A) and IHC staining (Fig. 2B). Lymphocyte accumulation in the portal area (portal-tract-associated lymphoid tissue; PALT) might be involved in extravasation of lymphocytes from vessels in the portal area, but

others demonstrated that DCs appeared in the sinusoidal wall and passed through the space of Disse to PALT, where the draining lymphatic duct is located.[14] There should be an active movement of immune cells between liver lobules and PALT, as reflected by the correlation of ISG expression in CLLs and CPAs in the MA patients of this study.

ISGs were reportedly up-regulated in hepatocytes of treatment-resistant IL28B genotype patients, but were up-regulated in Kupffer cells of treatment-sensitive genotype patients.[15] Our results confirmed these findings; however, we also showed that expression of various immune cell-surface markers, such as those on DCs, NK cells, macrophages, T cells, B cells, and granulocytes, was lower in MI than in MA patients (Supporting Fig. 5). In addition, we showed that expression of various chemokines was also repressed in MI patients, compared to MA patients (Supporting Fig. 4C-F).

Up-regulation of pretreatment chemokine (C-X-C motif) ligand 10/interferon-gamma-induced protein 10 (CXCL10/IP-10) serum levels is also associated with an unfavorable treatment outcome.[16] CXCL10 expression in the liver was significantly correlated with hepatic ISG expression and was higher in nonresponders than in responders (Supporting Fig. 10). Our results support the usefulness of serum CXCL10 for prediction of treatment outcome. Chemokine (C-X-C motif) receptor 3 (CXCR3) expression, a receptor for CXCL10, was inversely correlated with hepatic ISG expression and was significantly lower in MI than in MA patients (Supporting Fig. 10).

The lower number of immune cells in the liver lobules of MI patients would imply the reduced production of IFN from DCs, macrophages, and so on. Correlation analysis showed that hepatic ISGs were mainly associated with type III IFNs (IL28A/B and IL29), but not type I IFNs (IFN-α or IFN-β), although a significant association with IL29 was only observed in MA patients with up-regulated ISGs. This might be related to the high serum ALT levels in MAu patients (Fig. 3). Closer examination of hepatic ISGs and IL28A/B suggested that factors other than IL28A/B might regulate ISG expression in MI patients. During the preparation of this study, IFN-λ4 was newly identified to be expressed in hepatocytes from treatment-resistant IL28B genotype patients.[8] Interestingly, we found a significant correlation between hepatic ISGs and IFN-λ4 in MI patients (Fig. 3C). Moreover, a closer examination of gene expression profiling in MI patients enabled us to detect up-regulation of the noncanonical WNT ligand, WNT5A. RTD-PCR analysis of 168 patients confirmed up-regulation of WNT5A and its receptor, FZD5, in MI patients. Importantly, WNT5A expression was significantly correlated with hepatic ISG expression in MI patients. A recent report showed that WNT5A induces expression of ISGs, increases sensitivity of keratinocytes to IFN-α,[17] and might be involved in the immune response to influenza virus infection.[18] Therefore, we examined the role of WNT5A in hepatocytes. Interestingly, expression of WNT5A and ISGs was well correlated, and knocking down WNT5A using siRNA reduced expression of ISGs in THLE-5b cells (Supporting Fig. 8). Conversely, transduction of Huh-7 cells with WNT5A using a lentivirus system increased expression of ISGs. Despite the increase in ISG expression, WNT5A did not suppress HCV replication, but rather increased it in Huh-7 cells (Supporting Fig. 8). These results were also confirmed by using Huh-7 cells continuously infected with JFH-1. By knocking down or overexpressing WNT5A in Huh7-JFH1 cells, we showed that HCV-RNA was positively regulated by WNT5A (Fig. 5B,C).

WNT5A and its receptor, FZD5, mediate noncanonical WNT signaling, such as planar cell polarity and the WNT-Ca^{2+}-signaling pathway through G proteins. WNT5A reportedly inhibits B- and T-cell development by counteracting canonical WNT signaling.[19] We found that G3BP1, an SG assembly factor, was up-regulated by WNT5A (Fig. 5C). SGs were reportedly formed by endoplasmic reticulum stress, followed by HCV infection, and localized around lipid droplets with HCV replication complexes.[10] G3BP1 contributes to SG formation and increases HCV replication and infection in Huh-7 cells.[10] Moreover, a recent report demonstrated that G3BP1 is a DVL-associated protein that regulates WNT signaling downstream of the FZD receptor.[11] In this study, repression of WNT5A or FZD5 significantly reduced expression of DVL1-3, G3BP1, Mx1, and IFIT1 as well as HCV infectivity in Huh7-JFH1 cells (Fig. 5 and Supporting Fig. 9).

Importantly, we found a significant correlation between WNT5A and G3BP1 expression in liver tissue samples (Fig. 5E). We also found a significant correlation between FZD5 and G3BP1 expression in liver tissue samples (Fig. 5F). Thus, up-regulated noncanonical WNT5A-FZD5 signaling participates in the induction of ISG expression, but preserves HCV replication and infection in hepatocytes by increasing levels of the SG protein, G3BP1. These findings may explain the pathophysiological state of the treatment-resistant phenotype in MI patients.

In this study, we demonstrated impaired immune cell infiltration of the liver in treatment-resistant IL28B genotype patients, and we also demonstrated